Biochimica et Biophysica Acta 1862 (2016) 1–11

Contents lists available at ScienceDirect

Biochimica et Biophysica Acta

journal homepage: www.elsevier.com/locate/bbadis

Halofuginone promotes satellite cell activation and survival in muscular dystrophies

Hila Barzilai-Tutsch [a], Anna Bodanovsky [a], Hadar Maimon [a], Mark Pines [b], Orna Halevy [a,*]

[a] Department of Animal Sciences, The Hebrew University of Jerusalem, Rehovot 76100, Israel
[b] Institute of Animal Science, The Volcani Center, Bet Dagan 52505, Israel

ARTICLE INFO

Article history:
Received 7 July 2015
Received in revised form 5 October 2015
Accepted 6 October 2015
Available online 8 October 2015

Keywords:
Muscular dystrophy
Apoptosis
Cell cycle
Satellite cell
Myofiber
Halofuginone

ABSTRACT

Halofuginone is a leading agent in preventing fibrosis and inflammation in various muscular dystrophies. We hypothesized that in addition to these actions, halofuginone directly promotes the cell-cycle events of satellite cells in the *mdx* and *dysf*$^{-/-}$ mouse models of early-onset Duchenne muscular dystrophy and late-onset dysferlinopathy, respectively. In both models, addition of halofuginone to freshly prepared single gastrocnemius myofibers derived from 6-week-old mice increased BrdU incorporation at as early as 18 h of incubation, as well as phospho-histone H3 (PHH3) and MyoD protein expression in the attached satellite cells, while having no apparent effect on myofibers derived from wild-type mice. BrdU incorporation was abolished by an inhibitor of mitogen-activated protein kinase/extracellular signal-regulated protein kinase, suggesting involvement of this pathway in mediating halofuginone's effects on cell-cycle events. In cultures of myofibers and myoblasts isolated from *dysf*$^{-/-}$ mice, halofuginone reduced Bax and induced Bcl2 expression levels and induced Akt phosphorylation in a time-dependent manner. Addition of an inhibitor of the phosphinositide-3-kinase/Akt pathway reversed the halofuginone-induced cell survival, suggesting this pathway's involvement in mediating halofuginone's effects on survival. Thus, in addition to its known role in inhibiting fibrosis and inflammation, halofuginone plays a direct role in satellite cell activity and survival in muscular dystrophies, regardless of the mutation. These actions are of the utmost importance for improving muscle pathology and function in muscular dystrophies.

1. Introduction

The adult muscle tissue is composed of terminally differentiated mature myofibers [reviewed in 1,2]. In cases of acute stress such as injury, or under myopathic conditions, the myofibers' ability to regenerate and repair relies solely on the myogenic capacity of the muscle progenitor cells, the satellite cells [reviewed in 3]. These cells, normally quiescent, are situated in a niche between the sarcolemma and the basal lamina of the myofiber. In response to stress (e.g., mechanical stress, injuries, myopathies), appropriate stimulatory signals such as hepatocyte growth factor and nitric oxide (NO) [4–6] activate the satellite cells from their quiescent state. The cells are driven into the cell cycle and after several cell divisions, they exit the cell cycle and undergo myogenic differentiation, subsequently fusing with pre-existing or new myofibers [reviewed in 2,7].

In Duchenne muscular dystrophy (DMD), characterized by near absence of the protein dystrophin in skeletal muscles [8], the myofibers undergo repetitive cycles of degeneration–regeneration followed by a rise in inflammation and fibrosis and exhaustion of the satellite cell population [9,10, reviewed in 11]. For example, in a 9-year-old DMD patient, the proliferative life span of satellite cells was approximately one-third that of an age-matched control [12]. In contrast to DMD which evolves in early childhood, dysferlinopathy is an autosomal recessive late-onset MD with a mutation in the *dysferlin* gene that appears in patients between the ages of 20 to 30 years [13,14]. Though not characterized by the aggressive degeneration–regeneration cycles of DMD, similar cycles have been shown to occur along with a significant rise in inflammation and fibrosis [15–17].

Apoptosis has been shown to increase and become a leading cause of myofiber degradation following necrosis [reviewed in 18, 19] under acute stress such as electrical stimulation [20], in chronic conditions such as cachexia [21], in aging [22], and in MDs [11,23]. In *mdx* mice and DMD patients, upregulation of pro-apoptotic

Abbreviations: BrdU, 5-bromo-2′-deoxyuridine; CMD, congenital MD; DMD, Duchenne MD; DMEM, Dulbecco's Modified Eagle's Medium; ERK, extracellular signal-regulated protein kinase; DAPI, 4′,6-diamidino-2-phenylindole; MAPK, mitogen-activated protein kinase; MDs, muscular dystrophies; NO, nitric oxide; PI3K, phosphoinositide 3 kinase; PPH3, phospho-histone H3; TGFβ, transforming growth factor β; YY1, Ying-Yang 1.

* Corresponding author at: Dept. of Animal Sciences, The Hebrew University of Jerusalem, P.O. Box 12, Rehovot 76100, Israel.
E-mail address: orna.halevy@mail.huji.ac.il (O. Halevy).

http://dx.doi.org/10.1016/j.bbadis.2015.10.007
0925-4439/

proteins such as Bax and caspases has been observed in myofibers, suggesting that under pathological conditions, these myofibers undergo apoptosis [11]. Detection of apoptosis and decreased Bcl2 expression have been observed in patients with other MDs, such as Limb Girdle MD type 2C [24] and congenital MD (CMD) type 1A [25]. In agreement with others [11,19,21], we recently reported that in the *mdx* mouse model of DMD, the diaphragm, which is the muscle that is most affected by this disease, the number of apoptotic satellite cells and macrophages is higher than in wild-type mice [26]. In contrast, myofibroblasts, the activated form of fibroblasts, become resistant to apoptosis in dystrophic muscles [26–28]. Thus far, to the best of our knowledge, the presence of apoptosis has not been investigated in dysferlinopathies.

Halofuginone, an inhibitor of Smad3 phosphorylation downstream of the transforming growth factor β (TGFβ) signaling pathway, results in inhibition of the fibroblast-to-myofibroblast transition and fibrosis [29], reviewed in [30], and prolyl-tRNA synthetase activity results in inhibition of Th17 cell differentiation, thereby inhibiting inflammation [31,32]. Halofuginone has been reported to improve muscle histopathology in mouse models with early disease onset, such as *mdx* and the laminin α2-deficient dy^{2J}/dy^{2J} mouse model of CMD [33,34], reviewed in [35]. More recently, it has been reported that halofuginone also improves muscle histopathology and function in a dysferlin-knockout mouse model, through a direct effect on muscle cells. It promotes myotube fusion of primary myoblasts derived from normal and dystrophic muscles [36], and inhibits apoptosis of satellite cells and myofibers in the *mdx* mouse muscle [26]. Halofuginone promotes the phosphorylation of Akt and mitogen-activated protein kinase (MAPK) family members, and enhances the association of phosphorylated Akt and MAPK/extracellular signal-regulated protein kinase (MAPK/ERK) with the nonphosphorylated form of Smad3, resulting in decreased Smad3 phosphorylation [36]. Both MAPK/ERK and phosphoinositide 3 kinase (PI3K)/Akt pathways are involved in the myogenic lineage; the MAPK/ERK pathway has been reported to be mainly involved in early stages of myoblast proliferation [37,38], while the PI3K/Akt pathway has been shown to be crucial for later stages of their terminal differentiation and for cell survival [39–41].

The promotive effect of halofuginone on the MAPK/ERK pathway prompted us to look into its effect on cell-cycle events of satellite cells in mouse models of dysferlinopathy and DMD. Halofuginone promoted the entrance of single-myofiber-attached satellite cells into the cell cycle via the MAPK/ERK pathway. Moreover, the increased apoptosis in myofibers and myoblasts of the dysferlin-deficient mouse model was reduced by halofuginone treatment via the PI3K/Akt pathway.

2. Materials and methods

2.1. Reagents

Dulbecco's Modified Eagle's Medium (DMEM), sera and antibiotic-antimycotic solution were purchased from Biological Industries (Beit-Haemek, Israel). Ly294002 and UO127 were purchased from Calbiochem (Gibbstown, NJ). Halofuginone bromohydrate was obtained from Akashi Therapeutics, LLC (Newton, MA).

2.2. Mice

Male *dysf* $^{-/-}$ [mixed 129SvJ and C57/BL/g background (Stock 006,830) in which a 12-kb region of the *dysf* gene containing the last three exons is deleted, removing the transmembrane domain], *mdx* [C57BL/10ScSn-Dmd^{mdx}/J (Stock 001,801), dystrophin-deficient)] and C57/Bl/6 J (termed Wt or C57) mice (Jackson Laboratories, Bar Harbor, ME) were housed in cages under constant photoperiod (12 L:12 D) with free access to food and water. All animal experiments were carried out according to the guidelines of the Volcani Center Institutional Committee for Care and Use of Laboratory Animals (IL-234/10).

2.3. Cell preparation and maintenance

Primary myoblasts from the hind-leg muscles of 6-week-old mice were prepared as described previously [42]. Cells were plated at a low density of 3 x 10^5 in Petri dishes (90 mm diameter) to avoid spontaneous differentiation and grown at similar rate in DMEM supplemented with 20% (*v*/*v*) fetal calf serum (FCS) at 37.5 °C with humidified atmosphere and 5% CO_2 in air.

2.4. Single myofiber preparation and immunostaining

Single myofibers were isolated from the gastrocnemius muscle as described previously [26]. Briefly, six mice were sacrificed and the gastrocnemius muscles (6–7 muscles) were carefully removed. The outer connective tissue was removed and groups of three muscles were immersed in a 2.5-ml solution of 0.28% (*w*/*v*) collagenase type I in DMEM for 60 min for Wt and *mdx* mice, or for 90 min for *dysf* $^{-/-}$ mice. The collagenase-treated muscle was then transferred to horse serum (HS)-coated Petri dishes containing 10 ml of DMEM with 10% (*v*/*v*) HS for full coverage of the digested fibers, and triturated with a wide-mouth pipette. Myofibers were then washed three times with 10 ml DMEM with 10% HS and placed in 90-mm gelatin-coated plates and remained floating. Trypan blue staining revealed that almost 100% of these myofibers were viable (data not shown). For immunostaining, the myofibers were transferred to 35-mm plates, fixed with 4% paraformaldehyde and then incubated with Triton X-100 (0.5% *v*/*v* in PBS) and blocked with 20% (*v*/*v*) goat serum (GS) in PBS. The myofibers were incubated overnight at 4 °C with the following polyclonal antibodies: anti-Bax (1:150, Santa Cruz Biotechnology), anti-Bcl2 (1:150, Calbiochem), anti-phospho-histone H3 (PHH3), anti-phospho-Akt and anti-phospho-p42/44 (each at 1:1000 dilution, Cell Signaling, Beverly, MA), and monoclonal anti-MyoD (1:150, Santa Cruz Biotechnology), followed by incubation with Alexa 594 goat anti-rabbit IgG or Alexa 488 goat anti-rabbit IgG (1:300, Jackson Laboratories) secondary antibody for 1 h at room temperature. Nuclei were then stained with 4′,6-diamidino-2-phenylindole (DAPI; Sigma Aldrich, St. Louis, MO) in PBS. The myofibers were visualized under a fluorescence microscope (Olympus, Hamburg, Germany) with a DP-11 digital camera (Olympus). Negative control staining without the first antibody revealed some autofluorescence of the myofiber, but with no nucleus staining (data not shown).

2.5. 5-Bromo-2′-deoxyuridine (BrdU) incorporation

Single myofibers were cultured for 6 h in DMEM containing 10 μM BrdU (Sigma) and immunostained with mouse anti-BrdU antibody (G3G4, 1:2000, Becton Dickinson). Cultures were fixed in 2% paraformaldehyde for 15 min and then incubated with Triton X-100 (0.5% in PBS) and blocked with 5% GS and 1% HS in PBS. The cultures were incubated in 2 N HCl/0.2% Triton X-100 in double-distilled water for 10 min at room temperature followed by 5 min in 50 nM glycine in PBS. Incubation of myofibers with mouse anti-BrdU antibody was followed by incubation with biotinylated donkey anti-mouse IgG (1:250, Jackson Laboratories) for 1 h and in Texas Red streptavidin (1:300, Jackson Laboratories) for 30 min. Nuclei were stained with DAPI.

2.6. Western blot analysis

Western blot analysis was performed as described previously [43]. Briefly, equal amounts of protein (30 μg or 40 μg for myoblasts or

myofibers, respectively) were resolved by 10% SDS-PAGE and then transferred to nitrocellulose membranes (Bio-Rad). After blocking, the membranes were incubated with the following primary antibodies: rabbit polyclonal anti-Bax, rabbit polyclonal anti-Ying-Yang 1 (YY1, 1:500, Santa Cruz Biotechnology, Santa Cruz, CA), anti-Akt, anti-phospho-Akt, anti-phospho-p42/44 and anti-p42/44 (each at 1:1000, Cell Signaling). The secondary antibody used was polyclonal horse reddish peroxidase-conjugated goat anti rabbit (1:6000, Zymed, San Francisco, CA). Densitometric analysis was performed on bands using Gel-Pro Analyzer v3.0 software (Media Cybernetics Inc., Silver Spring, MD) software. Band intensity in each lane was normalized to the level YY1 as an internal standard [26].

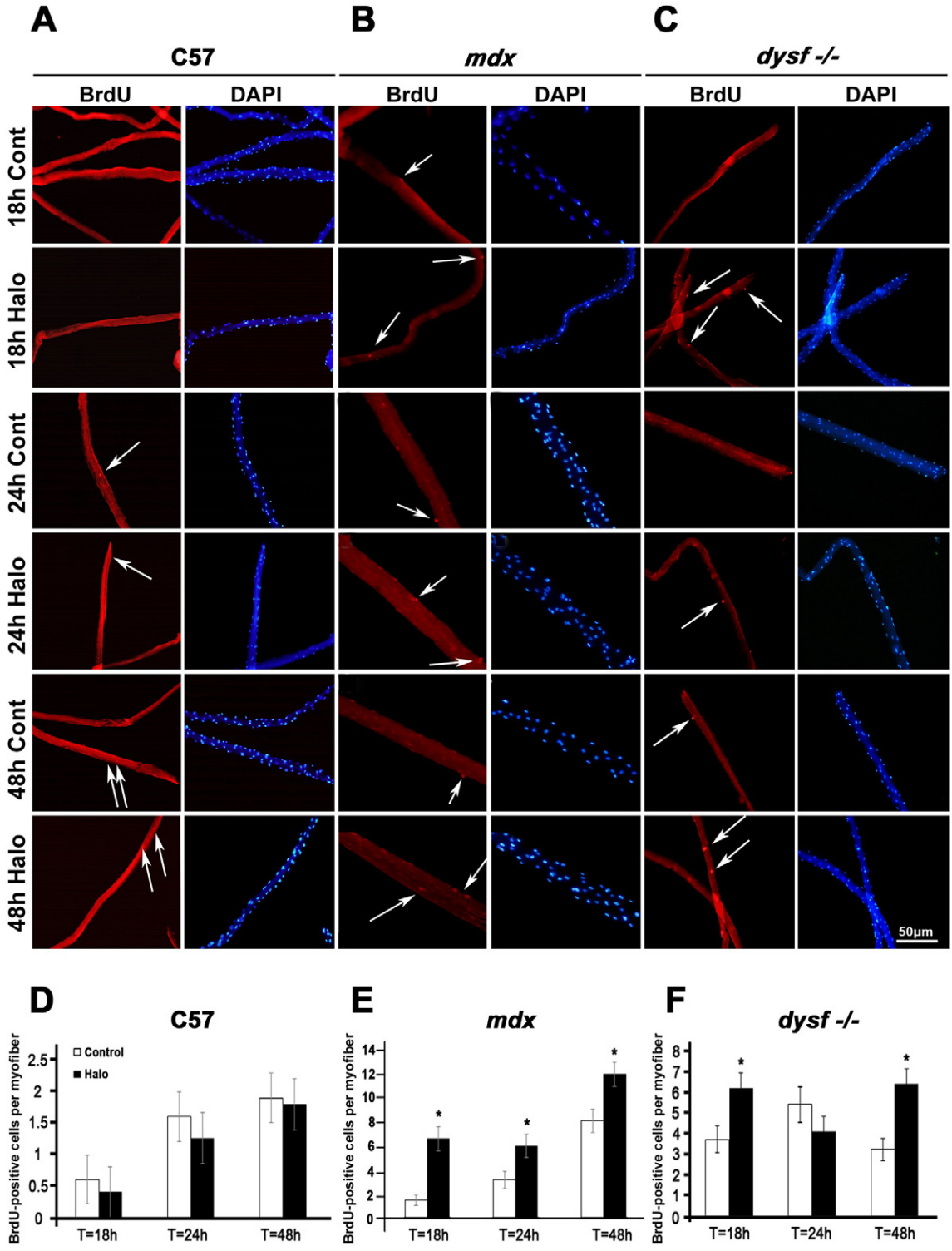

Fig. 1. BrdU expression in cells associated to myofibers derived from wild-type (C57; A), *mdx* (B) and *dysf*$^{-/-}$ (C) mice. Single myofibers isolated from the gastrocnemius of 6-week-old mice were untreated (Cont) or treated with 10 nM halofuginone (Halo) for 18, 24 and 48 h. BrdU (10 μM) was added for the last 6 h and then myofibers were stained for its presence. Nuclei were stained with DAPI. Arrows indicate BrdU-positive cells. Quantitation analysis of BrdU-positive cells in C57 (D), *mdx* (E) and *dysf*$^{-/-}$ (F) myofibers is presented as BrdU-positive cells per myofiber (n = 30 myofibers per treatment). *Significant difference within each time point at $P < 0.05$. Please note the different y-axis scales in D–F.

2.7. Statistical analysis

The data were subjected to one-way analysis of variance and to all-pairs Tukey-Kramer HSD test using JMP® software [44].

3. Results

3.1. Halofuginone increases cell-cycle activity and MyoD expression in cells associated with single dystrophic myofibers

Cell-cycle phases were evaluated using BrdU, a marker for DNA replication during the S-phase, and PHH3, a marker for M-phase entry. Single myofibers were prepared from the gastrocnemius muscle of 6-week-old Wt (C57), *mdx* and *dysf*$^{-/-}$ mice and were immediately treated, or untreated with 10 nM halofuginone for various times. BrdU was added for the last 6 h followed by immunofluorescence assay for its incorporation into DNA (Fig. 1).

Hardly any nuclei were stained for BrdU immediately after myofiber preparation (data not shown). After 18 h, a few BrdU-positive nuclei per myofiber were detected in all nontreated myofibers (Fig. 1A–C), suggesting the activation and cell-cycle entrance of single-myofiber-associated satellite cells [45,46]. Moreover, the number of BrdU-positive nuclei per myofiber increased at later time points in all myofibers (Fig. 1D-F), but was much lower in C57 vs. dystrophic myofibers. This was consistent with previous reports of Wt satellite cells being largely quiescent under steady-state conditions, as opposed to dystrophic muscles in which there is ongoing tissue regeneration due to genetic disorders [47–49]. Some reduction in *dysf*$^{-/-}$ BrdU-positive nuclei was observed after 48 h (Fig. 1F). The number of nuclei expressing BrdU in the halofuginone-treated C57 myofibers did not differ from that in the control untreated myofibers at any time point (Fig. 1A,D). However, single *mdx* myofibers treated with halofuginone demonstrated a significant rise in the number of BrdU-positive nuclei per myofiber relative to controls at all time-points, reaching approximately threefold already after 18 h of incubation (Fig. 1B,E). Halofuginone-treated *dysf*$^{-/-}$ myofibers demonstrated an approximately twofold rise in BrdU-positive nuclei per myofiber at 18 h and 48 h compared to controls, with no significant difference after 24 h (Fig. 1C,F).

Immunofluorescence staining for PHH3 in untreated single C57 and *dysf*$^{-/-}$ myofibers demonstrated an increase in PHH3-positive nuclei between 24 and 48 h of incubation (Fig. 2). Halofuginone treatment of C57 myofibers had no effect on the number of PHH3-positive cells per myofiber at either time point (Fig. 2B). However, in *dysf*$^{-/-}$ myofibers, a nearly significant increase ($P = 0.053$) in the number of PHH3-positive nuclei per myofiber was observed in response to halofuginone at 24 h compared to nontreated myofibers, which became significant at 48 h (Fig. 2C).

The expression of MyoD, a bona fide marker for activated satellite cells on isolated myofibers [45,46,50], was analyzed in *mdx* and *dysf*$^{-/-}$ myofiber nuclei in response to halofuginone. In freshly prepared myofibers, MyoD expression was observed in an average 1 nucleus per myofiber (data not shown). These numbers increased in all myofibers at 24 h and continued to rise at 48 h, confirming the activity of the attached satellite cells during the incubation periods (Fig. 3). The number of MyoD-positive nuclei per myofiber was approximately twofold higher in the halofuginone-treated *mdx* myofibers than in the control at both time points (Fig. 3B), and approximately 40% higher at 48 h in *dysf*$^{-/-}$ myofibers (Fig. 3C).

3.2. The increase in cell-cycle activity under halofuginone treatment is mediated via the MAPK/ERK pathway

The MAPK/ERK pathway is activated during early events of myoblast proliferation; it has been shown to be activated in *mdx* myoblasts and to mediate halofuginone's inhibitory effects on Smad3 phosphorylation [36]. We therefore evaluated whether this signaling pathway is affected by halofuginone in *dysf*$^{-/-}$ muscle cells as well, and whether it mediates the halofuginone-dependent cell-cycle activity of satellite cells in single myofibers. Single myofibers were derived from the gastrocnemius muscle of 6-week-old *dysf*$^{-/-}$ mice and immediately incubated, or not, with 10 nM halofuginone for 1 and 2 h. The single myofibers were fixed and reacted with antibody against the phosphorylated form of MAPK/ERK (Fig. 4A). Some myofiber-attached cells were already expressing phospho-MAPK/ERK at time zero (i.e., freshly prepared myofibers), suggesting some cell activity which could result from the preparation process. The number of cells expressing phospho-MAPK/ERK per myofiber increased within 1 h in the nontreated myofibers and remained the same at 2 h (Fig. 4B). In the halofuginone-treated myofibers, the number of cells expressing phospho-MAPK/ERK per myofiber was higher than that in nontreated ones at 1 h and remained higher at 2 h of incubation.

The effect of halofuginone on MAPK/ERK phosphorylation was also evaluated in primary myoblasts derived from *dysf*$^{-/-}$ mice at various time points. Phospho-MAPK/ERK levels (P-p42/44) were 2.2- and 2.5-fold higher in the halofuginone-treated cells than in controls after 60 and 120 min, respectively, and dropped back to control levels after 180 min (Fig. 4C). A combined treatment of halofuginone with UO126, a specific inhibitor of MAPK/ERK phosphorylation, for 60 min caused approximately threefold decrease in phospho-MAPK/ERK levels compared to halofuginone alone, down to the levels in nontreated myoblasts (Fig. 4D). Moreover, in *dysf*$^{-/-}$ myofibers treated with halofuginone for 18 h, the increase in BrdU-positive nuclei per myofiber was attenuated in the presence of UO126 (Fig. 4E); numbers remained comparable to those in control nontreated myofibers. This suggested that the MAPK/ERK pathway is required for halofuginone-induced satellite cell entrance into the cell cycle.

3.3. Halofuginone promotes the survival of cultured *dysf*$^{-/-}$ single myofibers and myoblasts

In light of the observed rise in cell-cycle markers in *dysf*$^{-/-}$ satellite cells, we tested whether halofuginone affects apoptosis levels in the *dysf* $^{-/-}$ muscle cells as it does in the *mdx* muscle [26]. Freshly prepared single myofibers derived from gastrocnemius muscle of 6-week-old *dysf*$^{-/-}$ mice were immediately incubated with or without 10 nM halofuginone for 24 h. The myofibers were fixed and reacted, side by side, with antibodies against the pro-apoptotic marker Bax and the anti-apoptotic marker Bcl2. The nontreated myofibers exhibited high levels of Bax (Fig. 5Aa), whereas the halofuginone-treated single fibers showed markedly decreased levels (Fig. 5Ac). A reciprocal effect was observed for Bcl2; its levels were low in the untreated myofibers (Fig. 5Ab) and increased in response to halofuginone (Fig. 5Ad). Western blot analysis of Bax levels (normalized to YY1) in these single myofibers revealed that halofuginone decreased Bax levels threefold compared to control nontreated myofibers (Fig. 5B). The high levels of Bax observed in single myofibers derived from untreated *dysf* $^{-/-}$ mice raised the possibility that their associated satellite cells undergo apoptosis, which is reduced by halofuginone. To test this, *dysf*$^{-/-}$ primary myoblasts were incubated for 24 h with or without halofuginone, and then analyzed for Bax protein levels (normalized to YY1; Fig. 5C). Densitometry analysis revealed that Bax levels were twofold lower in the halofuginone-treated cells compared to controls.

3.4. The increase in cell survival under halofuginone treatment is mediated by the PI3K/Akt pathway in *dysf*$^{-/-}$ muscle cells

Halofuginone has been shown to increase Akt phosphorylation levels in myoblasts [36], and to be required for muscle cell survival in *mdx* mice [26]. Single myofibers prepared from *dysf*$^{-/-}$ mice were immediately incubated with or without 10 nM halofuginone for 1 and 2 h, and immunostained for the phosphorylated form of

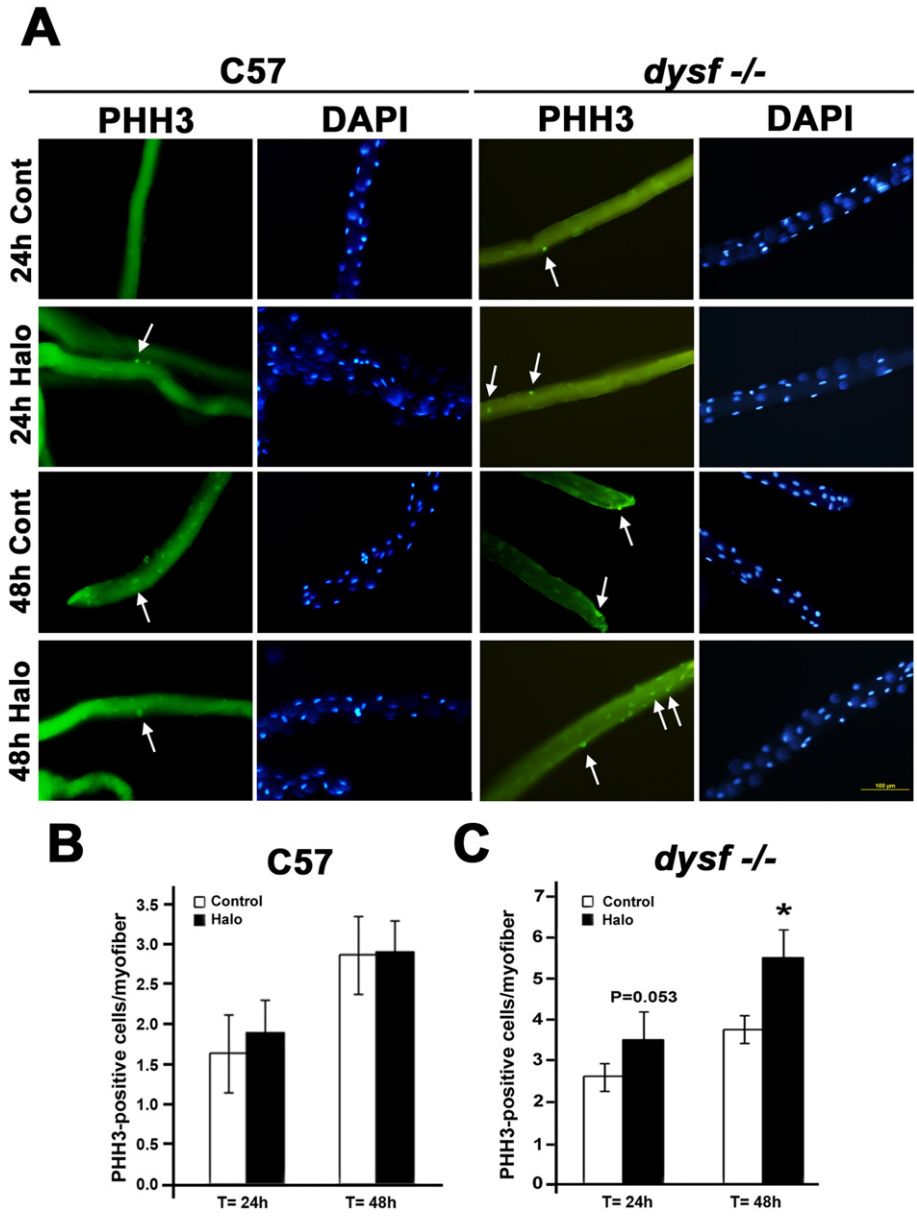

Fig. 2. PHH3 expression in cells associated with C57 and *dysf*$^{-/-}$ myofibers. Single myofibers prepared from gastrocnemius of 6-week-old C57 and *dysf* $^{-/-}$ mice were untreated (Control) or treated with 10 nM halofuginone (Halo) for 24 and 48 h, and then immunostained for PHH3. (A) Micrographs of single myofibers. Nuclei were stained with DAPI. Arrows indicate PHH3-positive nuclei, presumably satellite cells. (B) Quantitation analysis of PHH3-positive cells per myofiber in untreated and halofuginone-treated C57 myofibers. (C) Quantitation analysis of PHH3-positive cells in *dysf* $^{-/-}$ myofibers. In the 24 h treatment, the rise in the number of PHH3-positive cells treated with halofuginone was near significance ($P = 0.053$). *Significant difference at 48 h time point (n = 30; $P < 0.05$). Please note the different y-axis scales in B and C.

Akt. Phospho-Akt was observed in all cells, presumably satellite cells, on single myofibers at both time points (Fig. 6A). Whereas the number of phospho-Akt-positive cells in control myofibers remained constant at both time points (but significantly higher than at time 0), the number of phospho-Akt-positive cells was higher in halofuginone-treated vs. control myofibers at 1 h and continued to rise, becoming significantly higher after 2 h (Fig. 6B).

The level of phosphorylated Akt in the presence of halofuginone was evaluated in *dysf*$^{-/-}$ primary myoblasts at various time points. Akt phosphorylation levels were higher in the halofuginone-treated myoblasts at 60 min, and highest at 120 min relative to controls, then declined back to control levels at 180 min (Fig. 6C).

The requirement for the PI3K/Akt pathway in halofuginone-dependent cell survival was tested in *dysf* $^{-/-}$ primary myoblasts. Treatment with halofuginone for 60 min decreased Bax levels by half, whereas Akt phosphorylation levels increased 2.5-fold compared to those in the control untreated cells (Fig. 6D, E). However, the combined treatment of Ly294002, a specific inhibitor of Akt phosphorylation, with halofuginone abolished halofuginone's effect and caused a twofold increase in Bax levels compared to controls. Akt phosphorylation levels were reduced fivefold in control cells by Ly294002 addition, and over 15-fold in the presence of halofuginone compared to halofuginone-treated cells alone.

4. Discussion

Satellite cells are the main, if not the sole source for myoblasts in the regenerating muscle. As such, their ability to enter the cell-cycle and differentiate to myoblasts is of high importance for any injury in general and for MDs in particular. The results of this study show that halofuginone directly promotes cell-cycle progression of freshly isolated myofiber-attached satellite cells in the *mdx* mouse model for

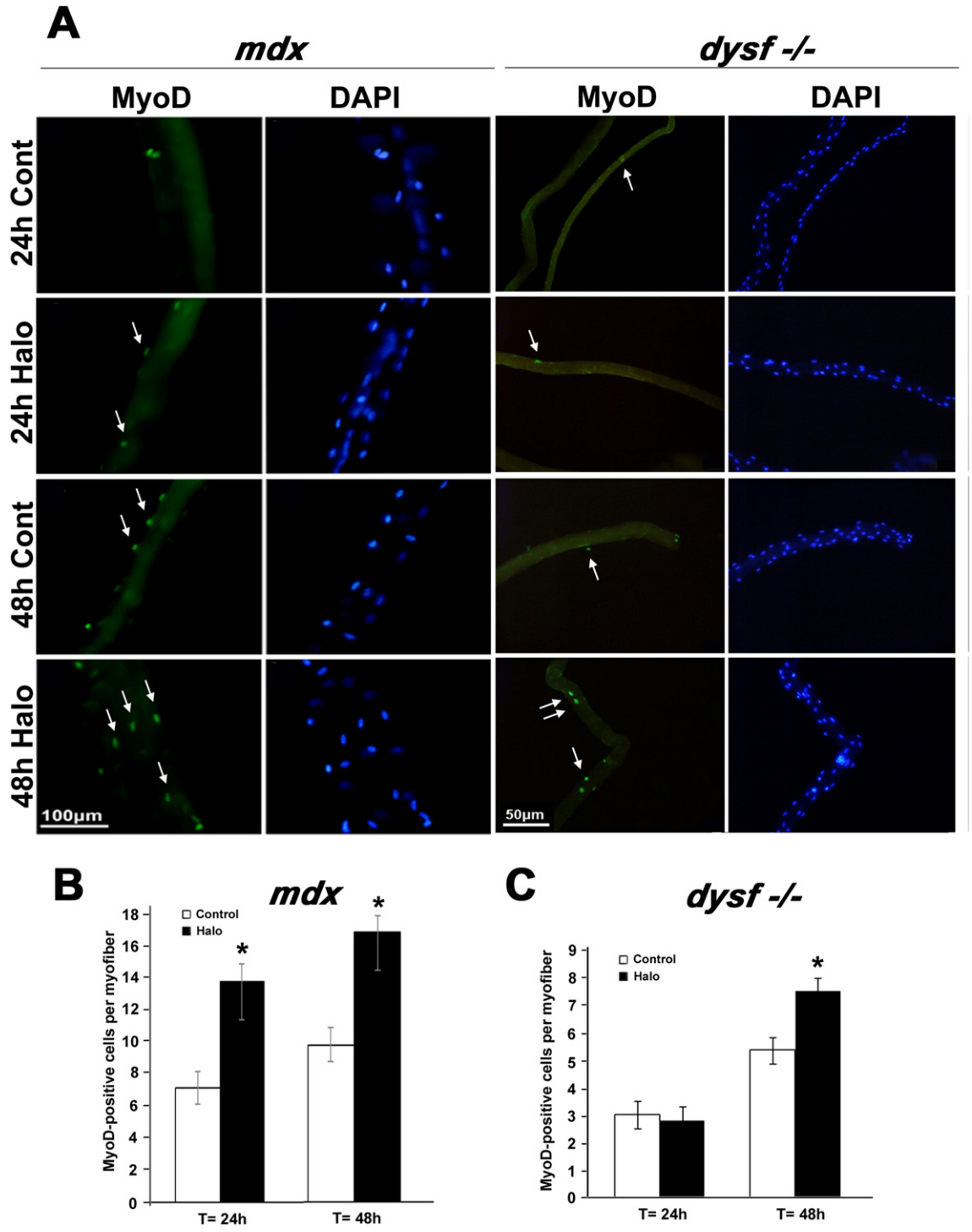

Fig. 3. Halofuginone increases the number of MyoD-positive nuclei on *mdx* and *dysf* $^{-/-}$ myofibers. (A) Micrographs of single myofibers derived from gastrocnemius of 6-week-old *mdx* and *dysf* $^{-/-}$ mice. Myofibers were untreated (Cont) or treated with 10 nM halofuginone (Halo) for 24 and 48 h, and then reacted with antibody against MyoD. Nuclei were stained with DAPI. Arrows indicate MyoD-positive nuclei. Note the abundance of MyoD-positive nuclei associated with the *mdx* myofiber in the 48 h Halo treatment. Quantitative analysis of MyoD-positive cells per myofiber in untreated and treated single myofibers derived from *mdx* (B) or *dysf* $^{-/-}$ (C) mice. *Significant difference within each time point (n = 30) at $P < 0.05$. Please note the different y-axis scales in B and C.

DMD – with early onset and severe fibrosis – and the *dysf*$^{-/-}$ mouse model for dysferlinopathy – with late onset and mild fibrosis. In addition, in support of our earlier studies using *mdx* mice [26], this study shows halofuginone's promotive effect on muscle cell survival in the *dysf*$^{-/-}$ mouse. Taken together, the results of this study suggest a direct positive role for halofuginone in ameliorating the pathology of dystrophic muscles, regardless of the mutation.

Cell-cycle activity of satellite cells was analyzed in single myofibers. Although cultured, these freshly prepared myofibers present the most accurate and in vivo-like cell system for investigations of satellite cell behavior [50]. In the dystrophic mice, the higher BrdU incorporation and PHH3 expression in the halofuginone-treated myofibers vs. controls, mark an increased effect of halofuginone on cell cycle events in the satellite cells [46,51]. No apparent effect of halofuginone

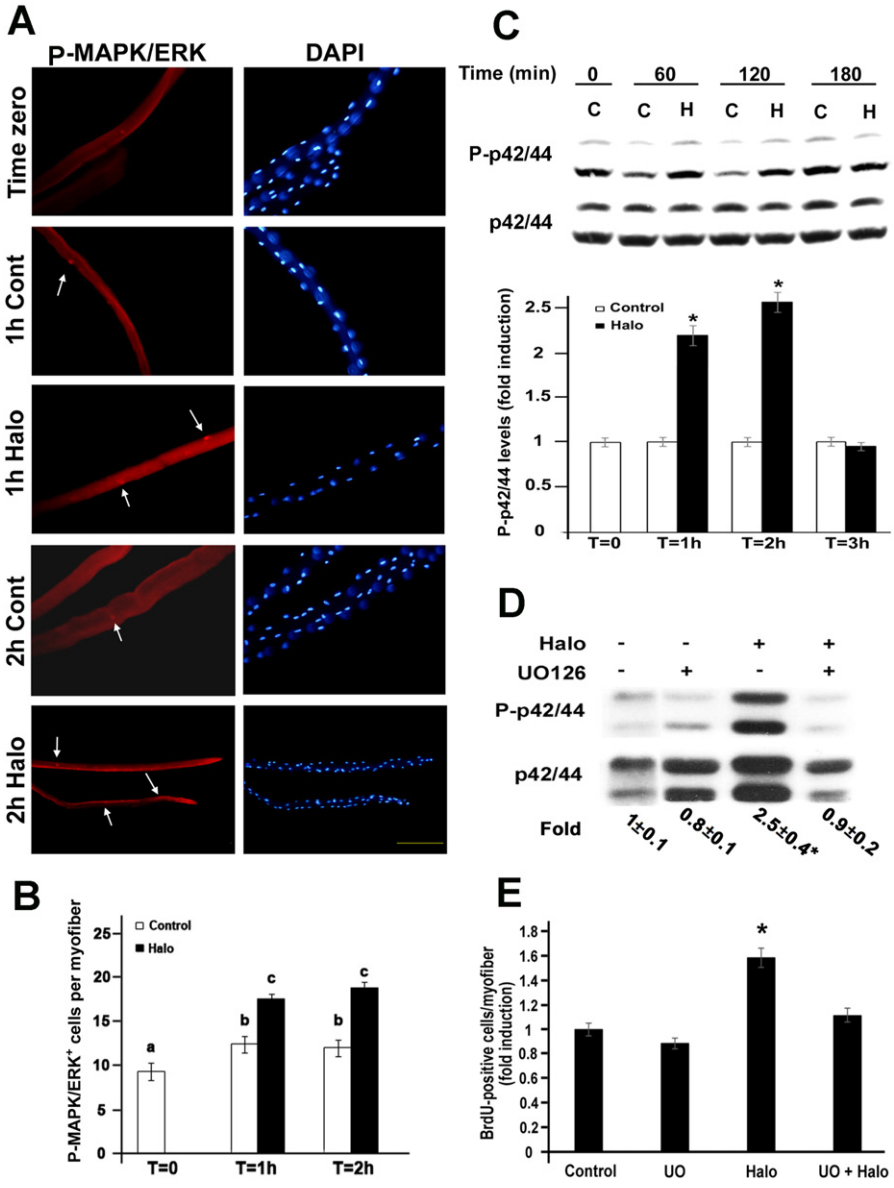

Fig. 4. Halofuginone increases the phosphorylation levels of MAPK/ERK in *dysf* $^{-/-}$ muscle cells. (A) Phosphorylated MAPK/ERK expression in single-myofiber-associated cells. Myofibers isolated from the gastrocnemius of 6-week-old mice were untreated (Cont) or treated with 10 nM halofuginone (Halo) for various times, and then immunostained for phospho-MAPK/ERK (P-MAPK/ERK). Nuclei were stained with DAPI. (B) Quantitation analysis of P-MAPK/ERK-positive cells (P-MAPK/ERK^{+}) per myofiber in control and halofuginone-treated *dysf*$^{-/-}$ myofibers (n = 30). Different letters represent statistically significant differences between all treatments at $P < 0.05$. (C) Myoblasts derived from hind-leg muscle of 6-week-old *dysf* $^{-/-}$ mice were incubated in the presence or absence of 10 nM halofuginone for various times, or in the presence or absence of UO126 (20 μM) for 60 min (D). Expression levels of phospho-MAPK/ERK (P-p42/44) were analyzed by Western blot. Densitometry analysis for levels of phosphorylated proteins was normalized to total p42/44 and is presented as fold induction relative to controls at each time point (C), or relative to control nontreated cells (D). C, Control; H, halofuginone. *Significant difference within treatments at $P < 0.05$ (n = 3). (E) The MAPK/ERK pathway is required for halofuginone-induced increase in BrdU incorporation. Myofibers were treated as in (A) with or without the addition of UO126 and/or halofuginone for 18 h. BrdU was added for the last 6 h and myofibers were then stained for BrdU presence in myofiber-attached nuclei. BrdU-positive nuclei were counted (n = 30 myofibers) and results are presented as fold induction of control nontreated myofibers. *Significant difference at $P < 0.05$. UO, UO126, Halo, halofuginone.

was observed on the nuclei of the Wt myofibers, suggesting a differential effect of halofuginone on satellite cells in favor of dystrophic muscles with chronic inflammation and fibrosis vs. Wt, in agreement with previous reports [17,33,34]. In addition, the cell cycle activity of satellite cells was reported to be higher in dystrophic muscles than in Wt muscles [47–49]. The promotive effect of halofuginone on the cell-cycle activity of satellite cells of dystrophic myofibers was also reflected in the higher number of nuclei expressing MyoD. MyoD and Myf5 are the first myogenic regulatory factors that mark the entrance of quiescent satellite cells into the myogenic program [46,52]. Together, the results suggest that halofuginone has the capacity to directly affect dystrophic myofibers and increase the cell cycle activity and myogenic proliferation of their attached satellite cells.

Some differences were noted in the myofibers derived from the different MD mouse models. More BrdU-positive nuclei were observed in the control *dysf*$^{-/-}$ vs. *mdx* myofibers at 18 h, which might be due to disease severity. At least with regard to dystrophin disorder, reduced cell-cycle entrance has been reported for DMD myoblasts [53] and for *mdx* myoblasts with severe phenotype [54]. Indeed, *mdx* muscle possesses reduced NO synthase activity, and thereby low production of NO which is crucial for satellite cell activation [5,6]. However, the different kinetics of BrdU incorporation and PHH3 expression in the *mdx* vs. *dysf*$^{-/-}$ myofiber-attached satellite cells implies a longer cell cycle in the latter. This longer cell cycle in *dysf*$^{-/-}$ cells could explain the mild or nonexistent effect of halofuginone on cell-cycle events and MyoD expression in these cells at 24 h, with a noticeable effect again

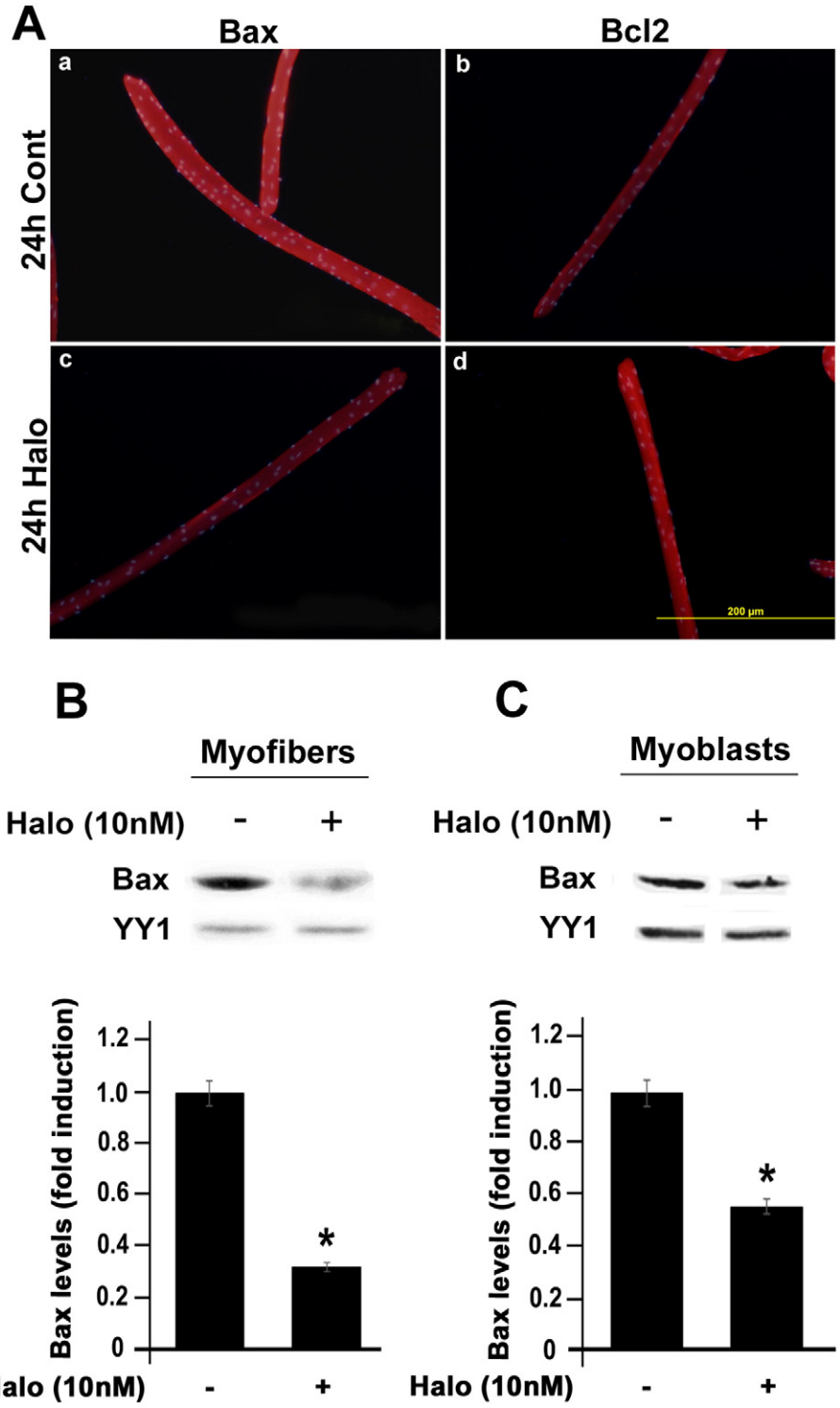

Fig. 5. Halofuginone's effect on the expression levels of pro- and anti-apoptotic markers in *dysf* $^{-/-}$ muscle cells. (A) Single myofibers were prepared from 6-week-old *dysf* $^{-/-}$ mice and immediately immunostained side by side for either Bax (a,c) or Bcl2 (b,d) under similar conditions. Nuclei were stained with DAPI. Note the lower Bax and higher Bcl2 intensity levels in myofibers treated with halofuginone and the reciprocal results in their untreated counterparts. Myofibers (B) or myoblasts (C) derived from *dysf* $^{-/-}$ gastrocnemius were untreated or treated with 10 nM halofuginone for 24 h. Bax protein levels in cell lysates were analyzed by Western blot. Densitometry analysis was normalized to total YY1 and is presented as fold induction relative to control. *Significant difference within treatments (n = 3) at $P < 0.05$.

at 48 h. Moreover, a major difference was noted in the extent of halofuginone's effect on cell-cycle markers and MyoD expression – being more profound in the *mdx* than *dysf*$^{-/-}$ mice. This implies a difference in the sensitivity of the satellite cells to halofuginone, which might be dependent on the genetic disorder and/or disease progression with regard to inflammation and fibrosis. The *mdx* mice exhibit an early-onset, severe phenotype at 6 weeks of age [33], the time of the single-myofiber preparation; on the other hand, the *dysf*$^{-/-}$ mice have a late-onset, mild phenotype, and while lacking the *dysferlin* gene, they still possess a structurally intact and stable dystrophin-glycoprotein complex in the muscles [55]. We previously reported a disparity between these two mouse models with regard to halofuginone's

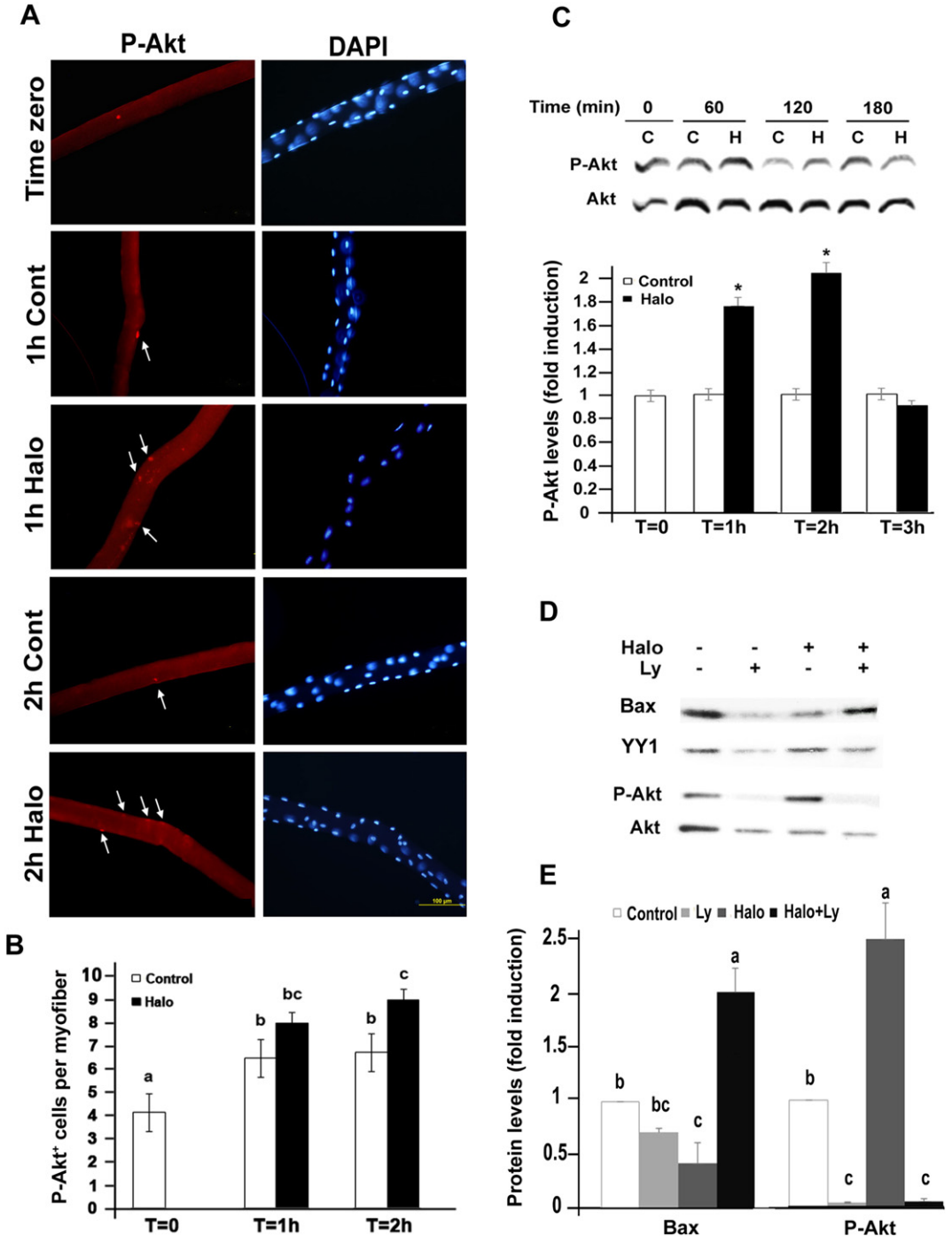

Fig. 6. Halofuginone increases Akt phosphorylation levels in single-myofiber-associated cells and primary myoblasts derived from *dysf* $^{-/-}$ mice. (A) Single myofibers derived from gastrocnemius of 6-week-old *dysf* $^{-/-}$ mice were untreated (Cont) or treated with 10 nM halofuginone (Halo) for 1 and 2 h, and then immunostained for phosphorylated Akt (P-Akt). Nuclei were stained with DAPI. Arrows indicate P-Akt-positive cells associated with the myofiber. (B) Quantitation analysis of P-Akt-positive cells (P-Akt^{+}) per myofiber in untreated and treated *dysf* $^{-/-}$ myofibers (n = 30). Different letters represent statistically significant differences ($P < 0.05$). (C) Myoblasts derived from hind-leg muscles of 6-week-old *dysf* $^{-/-}$ mice were incubated in the presence or absence of 10 nM halofuginone for various times. Phosphorylation levels of Akt were analyzed by Western blot. Densitometry analysis was normalized to total Akt and is presented as fold induction relative to control at each time point. *Significant difference within treatments (n = 3) at $P < 0.05$. C, Control; H, halofuginone. (D) *dysf* $^{-/-}$ myoblasts were incubated with or without halofuginone (10 nM) in the presence or absence of Ly294002 (Ly, 25 μM) for 60 min and the levels of Bax or phosphorylated Akt (P-Akt) were analyzed by Western blot. (E) Densitometry analysis for Bax and P-Akt was normalized to YY1 and total Akt, respectively. Results are presented as fold induction relative to controls (n = 3). Different letters represent statistically significant differences ($P < 0.05$).

effect on fibrosis and muscle functions, due to differences in disease progression [17].

Halofuginone has been reported to promote MAPK/ERK phosphorylation in *mdx* myoblasts [36]. The MAPK/ERK pathway has been reported to mediate myoblast proliferation [38,41]. Here, we demonstrate halofuginone's promotive effect on phospho-MAPK/ERK levels in satellite cells attached to freshly prepared single *dysf*$^{-/-}$ myofibers at as early as 1 h of incubation, suggesting halofuginone's effect on early cell-cycle events in these cells. The blockage of halofuginone-induced phosphorylation in *dysf*$^{-/-}$ myoblasts and BrdU incorporation in *dysf*$^{-/-}$ myofiber-attached satellite cells by a pharmacological MAPK/ERK inhibitor, UO126, suggest the requirement of this pathway

to mediate the effects of halofuginone on cell cycle progression. The phospho-MAPK/ERK pathway has been reported to mediate the inhibitory effect of halofuginone on the TGFβ/Smad3 pathway [36]; the latter pathway has been shown to interfere with the muscle's regenerative capacity [56] and myogenic proliferation [57,58].

In many MDs with sarcolemmal deficiencies, including CMD and DMD, apoptosis has been found to precede necrosis, the leading cause of myofiber degradation. A decline in apoptosis accompanied by a higher level of cell-cycle entrance can play a major role in improving muscle regeneration and function. Recently, halofuginone has been shown to increase the survival of satellite cells in the *mdx* muscle in vivo and in cultured primary myoblasts and isolated myofibers [26]. Here, we demonstrate a similar effect of halofuginone on the survival of freshly isolated myofibers and primary myoblasts derived from 6-week-old *dysf* $^{-/-}$ mice, before or at very early stages of the disease. This was reflected in: (a) the decline in Bax protein expression levels in myofibers and myoblasts, and upregulation of Bcl2 levels in myofibers to levels comparable to those derived from *mdx* mice (Fig. 5); (b) the time-dependent increase in Akt phosphorylation levels in *dysf* $^{-/-}$ single myofibers and primary myoblasts; (c) the requirement for the PI3K/Akt pathway to mediate halofuginone-induced effects on muscle cell survival. The PI3K/Akt pathway has been shown to attenuate apoptotic processes in various cell types, including skeletal muscle [59–61], and to be required for muscle cell survival in *mdx* mice [26]. Collectively, these and previous data suggest that the promotive effect of halofuginone on muscle cell survival is mediated by the PI3K/Akt pathway and is common to all MDs, regardless of their onset or progression rate.

Our previous and current results suggest that halofuginone's effects on muscle cell proliferation and survival are directly mediated by the MAPK/ERK and PI3K/Akt pathways. Nevertheless, it is conceivable that these pathways also indirectly affect halofuginone's actions, at least in part, via inhibition of the TGFβ/Smad3 pathway [36]. The TGFβ/Smad3 pathway has opposite effects on muscle cells and fibroblasts: it mediates the decrease in muscle cell survival and proliferation [58,62–64], but it is also involved in increasing the proliferation of fibroblasts and their differentiation to myofibroblasts, as well as their survival in dystrophic muscles [27,28,35]. These TGFβ/Smad3-mediated effects are inhibited by halofuginone in various tissues, including muscle [17,27,65,66], and therefore could explain this compound's differential and cell-type-specific effects on cell-cycle events and cell survival.

In conclusion, the data place halofuginone as an agent with a dual role in dystrophic muscle tissue. It functions as an anti-fibrotic agent regardless of the disease disorder, yet acts in a cell-specific manner with regard to cell-cycle progression and cell survival. Halofuginone inhibits cell proliferation and increases apoptosis of myofibroblasts, but it also enhances the cell-cycle activity of satellite cells along with muscle cell survival, regardless of MD type. The balance between these activities leads to the overall net effect of halofuginone on fibrosis, muscle regeneration and function. These effects are of the utmost importance as it is well known that in MDs in general, and in DMD in particular, repetitive cycles of degeneration–regeneration in a continuous attempt to deplete damaged myofibers and reconstruct healthy ones, exhaust the satellite cell population, impairing its proliferative or regenerative capacity.

Transparency Document

The Transparency Document associated with this article can be found, in the online version.

Acknowledgements

We thank Edouard Belauso for his help with the confocal microscopy. This study was supported in part by the Israel Science Foundation (ISF 1315/10).

References

[1] T.J. Hawke, D.J. Garry, Myogenic satellite cells: physiology to molecular biology, J. Appl. Physiol. 91 (2001) 534–551.
[2] Y.X. Wang, M.A. Rudnicki, Satellite cells, the engines of muscle repair, Nat. Rev. Mol. Cell Biol. 13 (2012) 127–133.
[3] G.Q. Wallace, E.M. McNally, Mechanisms of muscle degeneration, regeneration, and repair in the muscular dystrophies, Annu. Rev. Physiol. 71 (2009) 37–57.
[4] R. Tatsumi, J.E. Anderson, C.J. Neveret, O. Halevy, R.E. Allen, HGF/SF is present in normal adult skeletal muscle and is capable of activating satellite cells, Dev. Biol. 194 (1998) 114–128.
[5] A.C. Wozniak, J.E. Anderson, Nitric oxide-dependence of satellite stem cell activation and quiescence on normal skeletal muscle fiber, Dev. Dyn. 236 (2007) 240–250.
[6] J.E. Anderson, A role for nitric oxide in muscle repair: nitric oxide-mediated activation of muscle satellite cells, Mol. Biol. Cell 11 (2000) 1859–1874.
[7] P.S. Zammit, T.A. Partridge, Z. Yablonka-Reuveni, The skeletal muscle satellite cell: the stem cell that came in from the cold, J. Histochem. Cytochem. 54 (2006) 1177–1191.
[8] P.S. Harper, Gene mapping and the muscular dystrophies, Prog. Clin. Biol. Res. 306 (1989) 29–49.
[9] K.P. Campbell, S.D. Kahl, Association of dystrophin and an integral membrane glycoprotein, Nature 338 (1989) 259–262.
[10] K.A. Lapidos, R. Kakkar, E.M. McNally, The dystrophin glycoprotein complex: signaling strength and integrity for the sarcolemma, Circ. Res. 94 (2004) 1023–1031.
[11] D.S. Tews, Muscle-fiber apoptosis in neuromuscular diseases, Muscle Nerve 32 (2005) 443–458.
[12] V. Renault, G. Piron-Hamelin, C. Forestier, S. DiDonna, S. Decary, F. Hentati, G. Saillant, G.S. Butler-Browne, V. Mouly, Skeletal muscle regeneration and the mitotic clock, Exp. Gerontol. 35 (2000) 711–719.
[13] K.M. Bushby, Dysferlin and muscular dystrophy, Acta Neurol. Belg. 100 (2000) 142–145.
[14] L. Klinge, A. Aboumousa, M. Eagle, J. Hudson, A. Sarkozy, G. Vita, R. Charlton, M. Roberts, V. Straub, R. Barresi, H. Lochmüller, K. Bushby, New aspects on patients affected by dysferlin deficient muscular dystrophy, J. Neurol. Neurosurg. Psychiatry 81 (2010) 946–953.
[15] F. Barthélémy, N. Wein, M. Krahn, N. Lévy, M. Bartoli, M. Translational research and therapeutic perspectives in dysferlinopathies, Mol. Med. 17 (2011) 875–882.
[16] N. Gayathri, R. Alefia, A. Nalini, T.C. Yasha, M. Anita, M.V. Santosh, S.K. Shankar, Dysferlinopathy: spectrum of pathological changes in skeletal muscle tissue, Indian J. Pathol. Microbiol. 54 (2011) 350–354.
[17] O. Halevy, O. Genin, H. Barzilai-Tutsch, Y. Pima, O. Levi, I. Moshe, M. Pines, Inhibition of muscle fibrosis and improvement of muscle histopathology in dysferlin knock-out mice treated with halofuginone, Histol. Histopathol. 28 (2013) 211–226.
[18] D.S. Tews, Apoptosis and muscle fibre loss in neuromuscular disorders, Neuromuscul. Disord. 12 (2002) 613–622.
[19] J.G. Tidball, D.E. Albrecht, B.E. Lokensgar, M.J. Spencer, Apoptosis precedes necrosis of dystrophin-deficient muscle, J. Cell Sci. 108 (1995) 2197–2204.
[20] B.S. Guo, K.K. Cheung, S.S. Yeung, B.T. Zhang, E.W. Yeung, Electrical stimulation influences satellite cell proliferation and apoptosis in unloading-induced muscle atrophy in mice, PLoS One 7 (2012), e30348.
[21] S. Fulle, L. Centurione, R. Mancinelli, S. Sancilio, F.A. Manzoli, R. Di Pietro, Stem cell ageing and apoptosis, Curr. Pharm. Des. 18 (2012) 1694–1717.
[22] I. Michael, M.D. Lewis, Apoptosis as a potential mechanism of muscle cachexia in chronic obstructive pulmonary disease, Am. J. Respir. Crit. Care Med. 166 (2002) 434–436.
[23] M. Sandri, C. Minetti, M. Pedemonte, U. Carraro, Apoptotic myonuclei in human duchenne muscular dystrophy, Lab. Investig. 78 (1998) 1005–1016.
[24] I. Hadj Salem, F. Kamoun, N. Louhichi, M. Trigui, C. Triki, F. Fakhfakh, Impact of single-nucleotide polymorphisms at the TP53-binding and responsive promoter region of BCL2 gene in modulating the phenotypic variability of LGMD2C patients, Mol. Biol. Rep. 39 (2012) 7479–7486.
[25] M. Girgenrath, M.L. Beermann, V.K. Vishnudas, S. Homma, J.B. Miller, Pathology is alleviated by doxycycline in a laminin-alpha2-null model of congenital muscular dystrophy, Ann. Neurol. 65 (2009) 47–56.
[26] A. Bodanovsky, N. Guttman, H. Barzilai-Tutsch, O. Genin, O. Levy, M. Pines, O. Halevy, Halofuginone improves muscle-cell survival in muscular dystrophies, Biochim. Biophys. Acta 1843 (2014) 1339–1347.
[27] S. Zanotti, S. Gibertini, C. Bragato, R. Mantegazza, L. Morandi, M. Mora, Fibroblasts from the muscles of duchenne muscular dystrophy patients are resistant to cell detachment apoptosis, Exp. Cell Res. 317 (2011) 2536–2547.
[28] S. Zanotti, S. Gibertini, M. Mora, Altered production of extra-cellular matrix components by muscle-derived Duchenne muscular dystrophy fibroblasts before and after TGF-beta1 treatment, Cell Tissue Res. 339 (2010) 397–410.
[29] Y. Sheffer, O. Leon, J.H. Pinthus, A. Nagler, Y. Mor, O. Genin, M. Iluz, N. Kawada, K. Yoshizato, M. Pines, Inhibition of fibroblast to myofibroblast transition by halofuginone contribute to the chemotherapy-mediated anti-tumoral effect, Mol. Cancer Ther. 6 (2007) 570–577.
[30] M. Pines, Targeting TGFβ signaling to inhibit fibroblasts activation as a therapy for fibrosis and cancer, Expert Opin. Drug Discov. 3 (2008) 11–20.
[31] M.S. Sundrud, S.B. Koralov, M. Feuerer, D.P. Calado, A.E. Kozhaya, A. Rhule-Smith, R.E. Lefebvre, D. Unutmaz, R. Mazitschek, H. Waldner, M. Whitman, T. Keller, A. Rao, Halofuginone inhibits TH17 cell differentiation by activating the amino acid starvation response, Science 324 (2009) 1334–1338.
[32] T.L. Keller, D. Zocco, M.S. Sundrud, M. Hendrick, M. Edenius, J. Yum, Y.J. Kim, H.K. Lee, J.F. Cortese, D.F. Wirth, J.D. Dignam, A. Rao, C.Y. Yeo, R. Mazitschek, M. Whitman,

Halofuginone and other febrifugine derivatives inhibit prolyl-tRNA synthetase, Nat. Chem. Biol. 12 (2012) 311–317.
[33] T. Turgeman, K. Huebner, J. Anderson, O. Genin, A. Nagler, O. Halevy, M. Pines, Prevention of muscle fibrosis and improvement in muscle performance in the mdx mouse by halofuginone, Neuromuscul. Disord. 18 (2008) 857–868.
[34] Y. Nevo, O. Halevy, O. Genin, I. Moshe, T. Turgeman, M. Harel, E. Biton, S. Rief, M. Pines, Fibrosis inhibition and muscle characteristics improvement in laminin-α2 deficient mice, Muscle Nerve 42 (2010) 218–229.
[35] M. Pines, O. Halevy, Halofuginone and muscular dystrophy, Histol. Histopathol. 26 (2011) 135–146.
[36] S. Roffe, Y. Hagai, M. Pines, O. Halevy, Halofuginone inhibits Smad3 phosphorylation via the PI3K/Akt and MAPK/ERK pathways in muscle cells: effect on myotube fusion, Exp. Cell Res. 316 (2010) 1061–1069.
[37] S.A. Coolican, D.S. Samuel, D.Z. Ewton, F.J. McWade, J.R. Florini, The mitogenic and myogenic actions of insulin-like growth factors utilize distinct signaling pathways, J. Biol. Chem. 272 (1997) 6653–6662.
[38] N.C. Jones, Y.V. Fedorov, R.S. Rosenthal, B.B. Olwin, ERK1/2 is required for myoblast proliferation but is dispensable for muscle gene expression and cell fusion, J. Cell. Physiol. 186 (2001) 104–115.
[39] B.H. Jiang, M. Aoki, J.Z. Zheng, Z. Li, P.K. Vogt, Myogenic signaling of phosphatidylinositol 3-kinase requires the serine kinase Akt/protein kinase B, Proc. Natl. Acad. Sci. U. S. A. 96 (1999) 2077–2081.
[40] C. Rommel, S.C. Bodine, B.A. Clarke, R. Rossman, L. Nunez, T.N. Stitt, G.D. Yancopoulos, D.J. Glass, Mediation of IGF-1-induced skeletal myotube hypertrophy by PI(3)K/Akt/mTOR and PI(3)K/Akt/GSK3 pathways, Nat. Cell Biol. 11 (2001) 1009–1013.
[41] O. Halevy, L.C. Cantley, Differential regulation of the phosphoinositide 3-kinase and MAP kinase pathways by hepatocyte growth factor vs. insulin-like growth factor-I in myogenic cells, Exp. Cell Res. 297 (2004) 224–234.
[42] N. Ben Dov, G. Shefer, A. Irintchev, A. Wernig, U. Oron, O. Halevy, Low-energy laser irradiation affects satellite cell proliferation and differentiation in vitro, Biochim. Biophys. Acta 1448 (1999) 372–380.
[43] O. Halevy, Y. Piestun, M. Allouh, B. Rosser, Y. Rinkevitch, R.I. Rozenboim, M. Wleklinski-Lee, Z. Yablonka-Reuveni, The pattern of Pax7 expression during myogenesis in the posthatch chicken establishes a model for satellite cell differentiation and renewal, Dev. Dyn. 231 (2004) 489–502.
[44] SAS JMP, Statistics and Graphic Guide, Version 4, SAS Institute Incorporation, Cary, NC, 2002.
[45] Z. Yablonka-Reuveni, A.J. Rivera, Temporal expression of regulatory and structural muscle proteins during myogenesis of satellite cells on isolated adult rat fibers, Dev. Biol. 164 (1994) 588–603.
[46] D.D.W. Cornelison, B.J. Wold, Single-cell analysis of regulatory gene expression in quiescent and activated mouse skeletal muscle satellite cells, Dev. Biol. 191 (1997) 270–283.
[47] M. Cerletti, S. Jurga, C.A. Witczak, M.F. Hirshman, J.L. Shadrach, L.J. Goodyear, A.J. Wagers, Highly efficient, functional engraftment of skeletal muscle stem cells in dystrophic muscle, Cell 134 (2008) 37–47.
[48] K. Bockhold, J. Rosenblatt, T. Partridge, Aging normal and dystrophic mouse muscle: analysis of myogenicity in cultures of living single fibres, Muscle Nerve 21 (1998) 173–183.
[49] W. Duddy, S. Duguez, H. Johnston, T.V. Cohen, A. Phadke, H. Gordish-Dressman, K. Nagaraju, V. Gnocchi, S. Low, T. Partridge, Muscular dystrophy in the mdx mouse is a severe myopathy compounded by hypotrophy, hypertrophy and hyperplasia, Skelet. Muscle 5 (2015) 16, http://dx.doi.org/10.1186/s13395-015-0041-y.
[50] J.D. Rosenblatt, A.I. Lunt, D.J. Parry, T.A. Partridge, Culturing satellite cells from living single muscle fiber explants, In Vitro Cell. Dev. Biol. Anim. 3 (1995) 773–779.
[51] G. Shefer, T.A. Partridge, L. Heslop, J.G. Gross, U. Oron, O. Halevy, Low-energy laser irradiation promotes the survival and cell-cycle entry of skeletal muscle satellite cells, J. Cell Sci. 115 (2002) 1461–1469.
[52] A.S. Brack, T.A. Rando, Tissue-specific stem cells: lessons from the skeletal muscle satellite cell, Cell Stem Cell 10 (2014) 504–514.
[53] M.A. Melone, G. Peluso, O. Petillo, U. Galderisi, R. Cotrufo, Defective growth in vitro of duchenne muscular dystrophy myoblasts: the molecular and biochemical basis, J. Cell. Biochem. 76 (1999) 118–132.
[54] A. Sacco, F. Mourkioti, R. Tran, J. Choi, M. Llewellyn, P. Kraft, M. Shkreli, S. Delp, J.H. Pomerantz, S.E. Artandi, H.M. Blau, Short telomeres and stem cell exhaustion model duchenne muscular dystrophy in mdx/mTR mice, Cell 143 (2010) 1059–1071.
[55] Y.H. Chiu, M.A. Hornsey, L. Klinge, L.H. Jørgensen, S.H. Laval, R. Charlton, R. Barresi, V. Straub, H. Lochmüller, K. Bushby, Attenuated muscle regeneration is a key factor in dysferlin deficient muscular dystrophy, Hum. Mol. Genet. 18 (2009) 1976–1989.
[56] M.E. Carlson, M. Hsu, I.A. Conboy, Imbalance between pSmad3 and notch induces CDK inhibitors in old muscle stem cells, Nature 454 (2008) 528–532.
[57] H.J. You, M.W. Bruinsma, T. How, J.H. Ostrander, G.C. Blobe, Carcinogenesis. The type III TGF-beta receptor signals through both Smad3 and the p38 MAP kinase pathways to contribute to inhibition of cell proliferation, 282007 2491–2500.
[58] X. Li, D.C. McFarland, G.V. Velleman, Effect of Smad3-mediated transforming growth factor-beta1 signaling on satellite cell proliferation and differentiation in chickens, Poult. Sci. 87 (2008) 1823–1833.
[59] M.H. Kim, D.I. Kay, R.T. Rudra, B.M. Chen, N. Hsu, Y. Izumiya, L. Martinez, M.J. Spencer, K. Walsh, A.D. Grinnell, R.H. Crosbie, Myogenic Akt signaling attenuates muscular degeneration, promotes myofiber regeneration and improves muscle function in dystrophin-deficient mdx mice, Hum. Mol. Genet. 20 (2011) 1324–1338.
[60] R.T. Allen, K.D. Krueger, A. Dhume, D.K. Agrawal, Sustained Akt/PKB activation and transient attenuation of c-jun N-terminal kinase in the inhibition of apoptosis by IGF-1 in vascular smooth muscle cells, Apoptosis 10 (2005) 525–535.
[61] F. Mourkioti, N. Rosenthal, IGF-1, inflammation and stem cells: interactions during muscle regeneration, Trends Immunol. 26 (2005) 535–542.
[62] R.E. Allen, L.K. Boxhorn, Regulation of skeletal muscle satellite cell proliferation and differentiation by transforming growth factor-beta, insulin-like growth factor I, and fibroblast growth factor, J. Cell. Physiol. 138 (1989) 311–315.
[63] H.D. Kollias, J.C. McDermott, Transforming growth factor-β and myostatin signaling in skeletal muscle, J. Appl. Physiol. 104 (2008) 579–587.
[64] X. Li, D.C. McFarland, S. Velleman, Transforming growth factor-β1-induced satellite cell apoptosis in chickens associated with β1 integrin-mediated focal adhesion kinase activation, Poult. Sci. 88 (2009) 1725–1734.
[65] N. Haran, L. Leschinski, M. Pines, J. Rapoport, Inhibition of rat renal fibroblast proliferation by halofuginone, Nephron Exp. Nephrol. 104 (2006) 35–40.
[66] Y. Gnainsky, G. Spira, M. Paizi, R. Bruck, A. Nagler, O. Genin, R. Taub, O. Halevy, M. Pines, Involvement of the tyrosine phosphatase early gene of liver regeneration (PRL-1) in cell cycle and in liver regeneration and fibrosis effect of halofuginone, Cell Tissue Res. 324 (2006) 385–394.